INEEL/CON-02-00574
PREPRINT

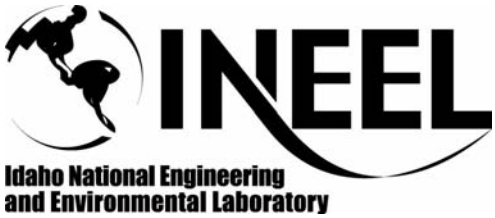


# Oxygen Reactivity of a Carbon Fiber Composite

T.D. Marshall, R.J. Pawelko, R.A. Anderl, G.R. Smolik, B.J. Merrill, R.L. Moore, D.A. Petti

## September 2002

## 22nd Symposium on Fusion Technology

# Oxygen Reactivity of a Carbon Fiber Composite

T.D. Marshall, R.J. Pawelko, R.A. Anderl, G.R. Smolik,
B.J. Merrill, R.L. Moore, D.A. Petti

Idaho National Engineering and Environmental Laboratory
P.O. Box 1625, Idaho Falls, ID 83415-3860 USA

**Abstract**

Carbon Fiber Composites (CFCs) are often suggested as armor material for the first wall of a fusion plasma chamber due to carbon's low atomic number, high thermal conductivity, and high melting point. However, carbon is chemically reactive in air and will react with ingress air during a Loss of Vacuum Accident and release tritium fuel that has been retained in the carbon. Tritium mobilization and carbon monoxide generation via CFC oxidation are both safety concerns.

This paper discusses chemical reactivity experiments that were performed using the state-of-the-art 3-dimensional NB31 CFC and a laminar reaction gas of Ar-21 vol% $O_2$. Oxidation reaction rates were measured for CFC temperatures of 525, 600, 700, 800, 900, and 1000 °C and a 100 standard cubic centimeters per minute (sccm) Ar-$O_2$ flow rate. Experiments were also performed at CFC temperatures of 700 and 1000 °C and a 1000 sccm Ar-$O_2$ flow rate. Mass spectral analyses of the exhaust reaction gas suggested that carbon monoxide was the primary reaction at the CFC surface and carbon dioxide was readily produced in the exiting reaction gas. The measured reaction rates compare well with the literature and were used to produce a CFC oxidation curve that is recommended for use in fusion safety analyses.

*Keywords*: CFC oxidation, carbon oxidation, oxidation experiment

## 1. Introduction

Literature [1] on the chemical reactivity of carbon suggests four potential chemical reactions between carbon and oxygen, as presented in Table 1.

Table 1. Chemical reactions between carbon and oxygen.

| Reaction | Free Energy (kcal) |
|---|---|
| $C(s) + O_2(g) = CO_2(g)$ | -94.03 |
| $C(s) + \frac{1}{2} O_2(g) = CO(g)$ | -26.62 |
| $CO(g) + \frac{1}{2} O_2(g) = CO_2(g)$ | -67.41 |
| $C(s) + CO_2(g) = 2CO(g)$ | +40.79 |
| **Note:** | (s) = solid; (g) = gas; CO = carbon monoxide; $CO_2$ = carbon dioxide |

The amount of carbon oxidized during the reactions in Table 1 and the amount of the product gases are highly dependent upon: oxygen concentration and flow rate, oxygen turbulence at the surface layer, and reaction temperature [2].

The negative free energies listed in Table 1 indicate that the reactions are chemically favorable. Accordingly, the free energy data in Table 1 suggest that the primary reaction of a CFC exposed to oxygen gas should produce carbon dioxide ($CO_2$) and carbon monoxide (CO). Thus, it was deemed important to measure the CO and $CO_2$ produced during the CFC-air chemical reactivity experiments.

Experiments on the chemical reactivity of carbon in an oxygen flow stream were previously performed by the Idaho National Engineering Laboratory (INEL) in 1988 [3]. Those experiments studied Union Carbide bulk graphite, FMI carbon-carbon composite graphite, and Pfizer pyrolytic graphite. The temperature range of those experiments was 800 to 1800 °C. The chemical reactivity experiments discussed here extend the 1988 data by using NB31, a state-of-the-art CFC frequently suggested for fusion applications, as the test specimen and testing over a temperature range of 525 to 1000 °C.

## 2. Fundamentals of carbon oxidation

In 1956, Rossberg and Wicke [4] performed graphite oxidation experiments and obtained results that suggested three discrete reaction regimes. These regimes are applicable for reactions between gases and porous solids with exclusively gaseous products [5].

Figure 1 illustrates the three kinetic regimes of chemical kinetic control (Regime I), in-pore diffusion of oxygen (Regime II), and boundary layer diffusion (Regime III). At low CFC temperatures, Regime I, the oxidizing gas homogeneously reacts with the porous CFC. Mass transport rates are more rapid than chemical reaction rates and an uniform oxidation occurs throughout the CFC. This regime involves chemisorption, chemical reaction, and desorption from internal surfaces; Regime I is uniquely controlled by the intrinsic chemical reactivity of the CFC.

Regime II oxidation occurs at a higher temperature than Regime I and features a heterogeneous reaction rate comprised of both surface chemical reaction and in-pore diffusion. Regime II is reported to have a lower temperature dependency than Regime I [6].

Regime III oxidation occurs at such a high temperature that the carbon is extremely reactive and thus the reaction rate is uniquely controlled by the oxygen mass transfer rate to the CFC surface. The oxygen mass transfer rate is strongly influenced by the nature of the gas at the CFC surface. For laminar flow, the mass transfer coefficient is dependent upon the diffusion coefficient [5], which increases with temperature to the 1.5 power [7].

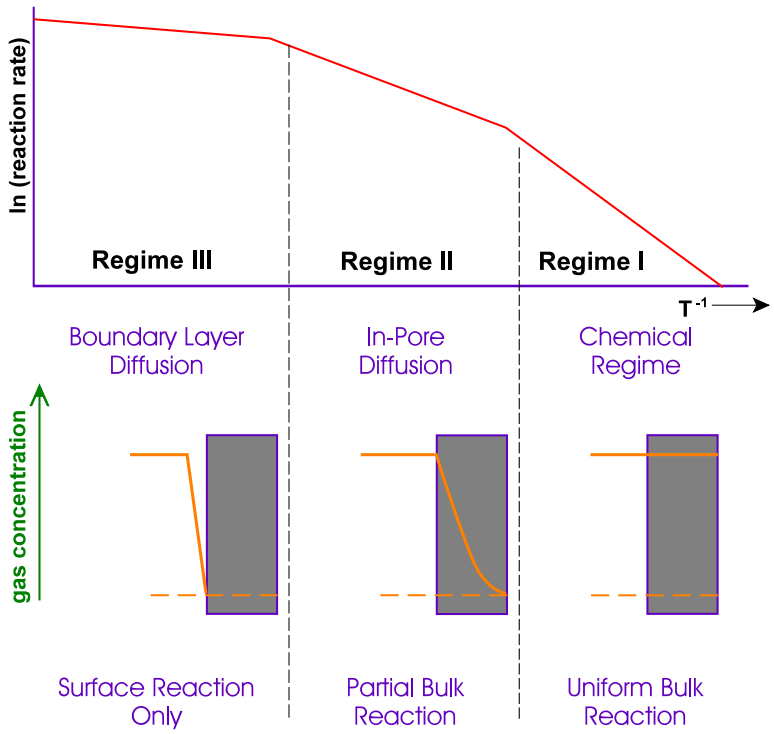


Figure 1. Schematic model of reactions between gases and porous CFC with exclusively gaseous products.

## 3. Test Specimen

NB31 [8] is an advanced, high thermal conductivity carbon fiber composite (CFC) that was manufactured by the Société Européenne de Propulsion and DUNLOP. An approximate density of 1.91 g/cm$^3$ was created by the processes of: (1) chemical infiltration of pyrocarbon at 1000 °C, (2) heat treatment at 2800 °C, (3) a second chemical infiltration of pyrocarbon at 1000 °C, and (4) a pitch impregnation at 100 MPa and 1000 °C. The dimensions of the test specimen were nominally 2.5 x 0.8 x 0.4 (L x W x D) cm.

## 4. Experiment System

The Idaho National Engineering and Environmental Laboratory (INEEL) Steam Reactivity Measurement System was originally assembled to measure hydrogen generation and tritium mobilization rates during steam interactions with irradiated beryllium [9]. For the CFC oxidation

experiments, the system was modified as shown in Figure 2. A reaction gas of Ar-21 vol% $O_2$ was used instead of ambient air because the $N_2$ gas in ambient air produces a mass signal of 28 on the mass spectrometer and would thereby mask the CO mass signal of 28.

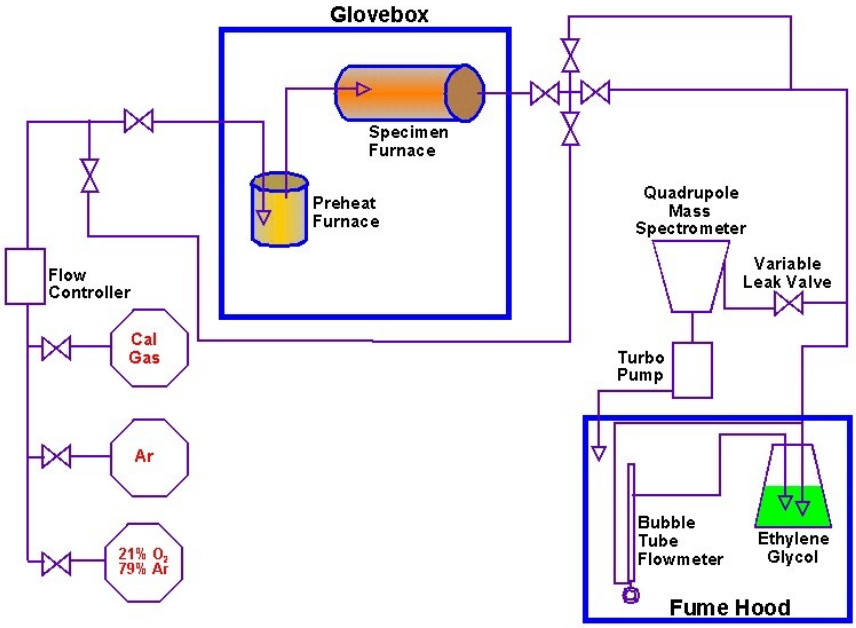


Figure 2: Schematic of INEEL chemical reactivity measurement system.

## 5. Experiment Procedure

The specimen was ultrasonically cleaned under inert gas, then weighed and installed in a quartz glass reaction chamber [10]. High purity Ar was circulated to purge the system of air and a quadropole mass spectrometer (QMS) sampled the exhaust Ar to verify that the system was without leaks. A tube furnace heated the quartz reaction chamber to the desired temperature and Ar-$O_2$ flowed through a pre-heater and into the quartz reaction chamber. The QMS measured the production of CO and $CO_2$ for the duration of the experiment. The reacted specimen was subsequently removed, weighed, and stored. The QMS provided CO and $CO_2$ concentration data as a function of reaction time, hence, those data provided kinetic information on CO and $CO_2$ generation rates. Integration of the QMS data yielded the total quantity of CO and $CO_2$ generated

while measurements of the specimen weight loss and the reaction time provided a determination of the oxidation rate.

## 6. Experiment Results

### *6.1 CO and $CO_2$ Generation Rates*

As a result of the low flow rate for the Ar-$O_2$ reaction gas, $CO_2$ was produced by the unconsumed $O_2$ reacting with the CFC surface-generated CO as the reaction gas exited the reaction chamber. The phenomenon explains the large amount of $CO_2$ measured during the experiment, see Table 2.

Table 2. CO and $CO_2$ data from NB31 chemical reactivity experiments.

| Specimen | Temp | C consumed | | CO produced | | $CO_2$ produced | |
|---|---|---|---|---|---|---|---|
| | (°C) | (mg) | (moles) | (std $cm^3$) | (moles) | (std $cm^3$) | (moles) |
| **100 std-$cm^3$ Ar-$O_2$ Flow Rate** | | | | | | | |
| NB31-08 | 525 | 4.1 | 0.0003 | 7.4 | 0.0003 | 9.2 | 0.0004 |
| NB31-02 | 601 | 30.6 | 0.0026 | 15.5 | 0.0007 | 68.2 | 0.0030 |
| NB31-01 | 705 | 663.2 | 0.0552 | 334.2 | 0.0149 | 1202.9 | 0.0537 |
| NB31-04 | 815 | 356.2 | 0.0297 | 3.7 | 0.0002 | 828.4 | 0.0370 |
| NB31-05 | 919 | 165.6 | 0.0138 | 2.8 | 0.0001 | 394.9 | 0.0176 |
| NB31-03 | 1016 | 92.1 | 0.0077 | 0.0 | 0.0000 | 231.4 | 0.0103 |
| **1000 std-$cm^3$ Ar-$O_2$ Flow Rate** | | | | | | | |
| NB31-09 | 705 | 71.1 | 0.0059 | 39.0 | 0.0017 | 112.1 | 0.0050 |
| NB31-06 | 1054 | 344.7 | 0.0287 | 4.7 | 0.0002 | 730.0 | 0.0326 |
| **3 std-$cm^3$ Ar-$O_2$ Flow Rate** | | | | | | | |
| NB31-07 | 705 | 115.0 | 0.0096 | 4.7 | 0.0002 | 249.6 | 0.0111 |

*6.2 Reaction Rates*

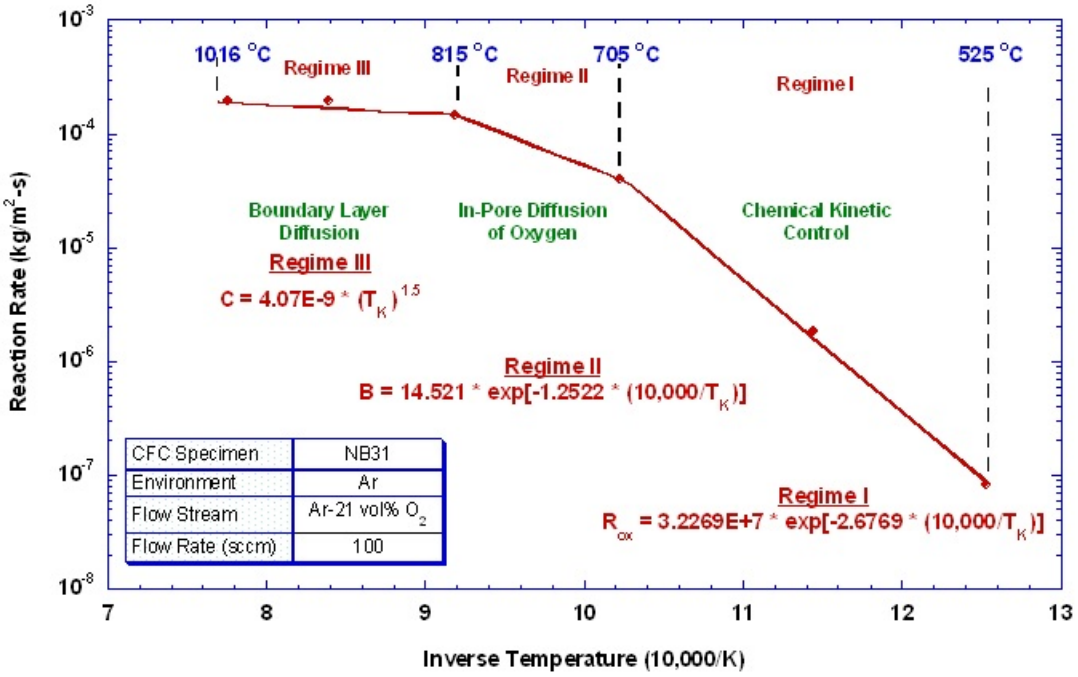


Figure 3. Experiment reaction rates with curve fit and identification of oxidation regimes.

The calculated reaction rates, defined as CFC weight loss (kg) divided by the product of the CFC geometric surface area ($m^2$) and the oxidation time (s), are presented in Figure 3. The three regimes of oxidation were identified using the change in slope for the linear curve fits applied to the experiment data.

*6.3 Integrated Reaction Rates*

Integration of the previous INEL carbon oxidation experiments with the current experiment data produces a CFC oxidation curve that is recommended for use in fusion safety analyses:

Regime I: [525 ≤ T < 710 °C]

$$R_{ox} = 1.4754 \times 10^{7} \cdot \exp\left[-2.6128 \cdot \frac{10000}{T_K}\right] \quad \textbf{(1)}$$

Regime II: [710 ≤ T < 1175 °C]

$$R_{ox} = 36.308 \cdot \exp\left[-1.3475 \cdot \frac{10000}{T_K}\right] \quad \textbf{(2)}$$

Regime III: [1175 ≤ T < 1720 °C]

$$R_{ox} = 1.57 \times 10^2 \cdot \exp\left[-0.226 \cdot \frac{10000}{T_K}\right] \quad \textbf{(3)}$$

## 7.0 Conclusions

Oxidation experiments with the NB31 state-of-the-art CFC were performed to supplement previous oxidation data. The new data exhibited the traditional three regimes of oxidation, and when integrated with the previous data, produced an oxidation curve that should adequately predict CFC oxidation in the first wall of a fusion plasma chamber.

## 8.0 References


1. Advances in Catalysis and Related Subjects, Volume XI, Academic Press Inc., 1959, pp 133-217.

2. L. Snead and T. Burchell, "Oxidation of High-Quality Graphite for IFE," Proceedings of the DOE/NE High Average Power Laser Program Workshop, Pleasanton, CA, July 25-26, 2002.

3. M.H. O'brien, B.J. Merrill, and S.N. Ugaki, Combustion Testing and Thermal Modeling of Proposed CIT Graphite Tile Materials, INEL, EGG-FSP-8255, 1988.

4. M. Rossberg and E. Wicke, "Transportvorgänge und Oberflächenreaktionen bei der Verbrennung graphitischen Kohlenstoffs," Chemie-Ingenieur-Technik, 3, pp 181-189, 1956.

5. R. Moormann, "Graphite Oxidation Phenomena During Massive Air Ingress Accidents in Nuclear High Temperature Gas Cooled Reactors with Pebble Bed Core," Berichte der Bunsen-Gesellschaft fur Physikalische Chemie, 87, 11, 1983, pp 1086-1090.

6. R.P. Wichner and S.J. Ball, Potential Damage to Gas-Cooled Graphite Reactors Due to Severe Accidents, ORNL/TM-13661, Oak Ridge National Laboratory, 1999, Appendix A.

7. J.R. Welty, C.E. Wicks, R.E. Wilson, Fundamentals of Momentum, Heat and Mass Transfer, John Wiley & Sons, New York, 1969, pg 455.

8. J-P Bonal and D Moulinier, Thermal Properties of Advanced Carbon Fiber Composites for Fusion Application, Commissariat A L'Energie Atomique, Rapport DMT/95-495, October 1995.

9. G.R. Longhurst et. al., Fusion Safety Program Annual Report Fiscal Year 1996, INEEL, INEL-96/0483, pp 11-12, December 1996.

10. T.D. Marshall, R.J. Pawelko, R.A. Anderl, G.R. Smolik, B.J. Merrill, R.L. Moore, Air Chemical Reactivity Measurements of the Carbon Fiber Composite NB31, INEEL, INEEL/EXT-02-00745, May 2002.